Effects of some air-jet impingement parameters on the removal of seeds from sunflower heads in linear movement

Amir Hossein Mirzabe[1,*], Golam Reza Chegini[2], Jafar Massah[2], Javad Khazaei[2]

(*1. Department of Mechanical Engineering of Biosystems, Faculty of Agricultural Engineering and Technology, College of Agriculture & Natural Resources, University of Tehran, Tehran, Iran*

2. Department of Mechanical Engineering of Biosystems, College of Aboureihan, University of Tehran, Tehran, Iran)

Abstract: Due to the success of air-jet application in food and agricultural sciences, a new method was invented based on the impingement jets to eliminate some problems presented in mechanical methods of removing sunflower seeds from the head. When the sunflower head had linear velocity and the nozzle was fixed, the effects of the seeds' location on the sunflower head, reservoir pressure, nozzle diameter, linear velocity of the sunflower head, and the distance between the nozzle outlet and the surface of the sunflower head on its removed area were examined. The regions removed by the impingement of the air-jet were photographed, and the area of the removed regions was calculated based on the image processing technique. The results showed that the area of the removed region increased with increasing the nozzle diameter, reservoir pressure, and distance between the nozzle outlet and sunflower head; also, the area of the removed region increased with decreasing the linear velocity of the sunflower head. The maximum value of the area of the removed region in all regions was obtained when the linear velocity, nozzle diameter, reservoir pressure, and distance between nozzle outlet and sunflower head were equal to 1 cm sec^{-1}, 8 mm, 800 kPa, and 30 mm, respectively. The minimum value of the area of the removed region in all regions was obtained when the linear velocity, nozzle diameter, reservoir pressure, and distance between nozzle outlet and sunflower head were equal to 3 cm sec^{-1}, 4 mm, 600 kPa, and 10 mm, respectively.

Keywords: sunflower, thresher machine, image processing, linear velocity, power consumption, energy consumption

Citation: Mirzabe, A. H., G. R. Chegini, J. Massah, and J. Khazaei. 2021. Effects of some air-jet impingement parameters on the removal of seeds from sunflower heads in linear movement. Agricultural Engineering International: CIGR Journal, 23(2):111–129.

1 Introduction

Sunflower (*Helianthus annuus* L.) is one of the most important oil crops due to its high amount of unsaturated fatty acids and the absence of cholesterol (Razi and Assad, 1998; Darvishzadeh et al., 2010). It originated from North America. It was selected for its high oil in Russia in 1860, and Russia was largely responsible for increasing oil content from 28% to almost 50% (Mirzabe et al., 2014). Sunflower oil has a light color, bland flavor, high smoke point, and a relatively high concentration of polyunsaturated fatty acid and linoleic acid (Mirzabe and Chegini, 2015).

The area under sunflower has increased by more than 15 times during the last fifteen years, indicating strong farmers' motivation of the state for this crop (Goel et al., 2009). Despite increasing in the area under sunflower

Received date: 2019-12-29 **Accepted date:** 2021-03-28

***Corresponding author: Amir Hossein Mirzabe,** Ph.D Candidate. Department of Mechanical Engineering of Biosystems, Faculty of Agricultural Engineering and Technology, College of Agriculture & Natural Resources, University of Tehran, Tehran, Iran, Tel: 098 3153239185, Fax: +98-21-36040614, Email: ah_mirzabe@alumni.ut.ac.ir or ah_mirzabe@yahoo.com

production in many developing countries, there are many problems for planting sunflowers such as pest's damage, diseases damage, poor soil fertility, water pressure (Nderitu et al., 2008), and non-availability of suitable machinery for sunflower's sowing, harvesting, post-harvesting, and oil extraction operations. For example, Iran relies heavily on the imports of edible oil to make up for the low production levels of oil crops as they cannot meet the growing demands of oil factories. While there are suitable conditions and reasons for sunflower cultivation in Iran, in most areas, it is usually cultivated in small farms. In some developing countries like Iran, one of the most important reasons for not cultivating sunflower is non-availability of suitable machinery for its harvest, post-harvest and, oil extraction operations (Mirzabe and Chegini, 2016).

Nowadays, there are two methods for removing sunflowers seeds from their heads, 1) traditional or manual method and, 2) mechanized mechanical method. The efficiency of the manual methods depends on the efficiency and experience of the workers, and it is deficient (Mirzabe et al., 2012; Goel et al., 2009). The mechanical methods of removing sunflower seeds are based on beating, friction, and simultaneous beating and friction. Although several studies have been conducted on threshing sunflower (Anil et al., 1998; Bansal and Dahiya, 2001; Sharma and Devnani, 1979; Sudajan et al., 2005; Sudajan et al., 2003) to reduce the number of damaged seeds, and also decrease the power consumption and increase the efficiency of thresher machines, these machines are not suitable yet.

Nowadays, air and water-jets impingements have many applications in industry, food sciences, and agriculture. One of the most critical applications of impingement jets is heat or mass transfer. Impinging jet is widely used in thermal industrial applications due to its high heat transfer coefficient in the impingement region (Yeranee et al., 2017). It seems that the most practical aspect of the jets is the mass or heat transfer, and there are a lot of scientific works in this field (Zuckerman and Lior, 2006; Webb and Ma, 1995; Viskanta, 1993; Rodi, 2014; Polat, 1993; Martin, 1977; Huang and El-Genk, 1994; Goldstein et al., 1986; Gardon and Akfirat, 1966).

Due to the success of the application of air-jet in removing arils of pomegranate fruits and extracting citrus juice and juice sacs (Ando et al., 1988; Hayashi et al., 1981; Khazaei et al., 2008a; Khazaei et al., 2008b; Nahir and Ronen, 1992; Sarig et al., 1985; Schmilovitch et al., 2014), in order to eliminate a number of problems in manual and mechanical methods of removing sunflower seeds from the head, a new method was invented based on the impingement air-jets.

The model of this machine was preliminarily designed, constructed, and evaluated by Mirzabe et al. (2014). Although this preliminarily manufactured remover machine had a good and acceptable performance, the aim of presenting the air-jet impingement method was not to design this simple machine. The final machine was supposed to take a sunflower with all its seeds from one end, deliver the empty flower, and separated seeds on its other end. In the design of the final machine, the sunflower head should have a linear velocity and, simultaneously, nozzles should have a rotational velocity. Combining these two velocities (linear velocity of sunflower head and rotational velocity of the nozzles) causes the seeds located in different regions of the sunflower head to become subjected to the jet force, hence getting removed. Although the manufactured machine plays an efficient role in recognizing the jet parameters and their effects on the sunflower heads and seeds, the results obtained from the preliminary machine are not enough, and we need to study the jet parameters in other simple states. In the machine manufactured in 2014 by Mirzabe et al. (2014), the effects of rotational velocity of the nozzles were studied. In the current study, the effect of the linear velocity of the sunflower head is studied to attain thorough knowledge on the effects of the air-jet on the seeds in different conditions for designing the final sunflower seeds remover machine.

The aim of the present study is, therefore, to investigate the effects of the Pressure of Compressor Reservoir (PCR), the distance between nozzle outlet and sunflower head

surface (DNS), Nozzle Output Diameter (NOD), the linear velocity of sunflower head (LVS), and seeds location on the head on removing sunflower seeds from their head when the sunflower head has linear velocity, and the nozzle is fixed. All considered parameters and their ranges chose based on theoretical calculations, some pretests, and previous experiences in this regard. Also, the theoretical area of the covered region by air-jet in different levels of distance between nozzle outlet and sunflower head surface and nozzle diameter was calculated and compared to the experimental area of the removed region by air-jet. In addition, Area of Removed Region (ARR) was modeled in each region of the sunflower head using linear and quadratic functions, and ARR was optimized using Response Surface Methodology (RSM).

2 Materials and methods

2.1 Sampling preparation

The "*Shamshiri*" variety of sunflowers, being widely cultivated in Iran, was used in the present study. This variety is native to Iran. The sunflowers were planted on April 27th, 2012, in research farms of the University of Tehran located in Pakdasht, Tehran Province, Iran (longitude of 35.47° N, latitude of 51.67° E, average annual precipitation of 110 mm from 2000 to 2010, height above the sea level of 1025 m, and average annual temperature of 18.0℃ from 1993 to 2010). The sunflowers of the mentioned variety were harvested manually in late September when SHs (Sunflower Heads) were utterly matured.

2.2 Theoretical calculations

For removing the sunflower seeds from the SH (Sunflower Head) using air-jet impingement, seeds were subjected to external forces caused by the air-jet. The high-speed air-jet transfers momentum to the SH and sunflower seeds and generates forces on the head surface. Calculation of the force available from a given jet requires knowledge of the local speed of sound, critical speed of sound, many numbers, air density in the reservoir, ambient pressure, pressure of compressor reservoir, and the nozzle diameter. Also, calculation of the covered region by air-jet requires knowledge of the gas discharging and the jet formation.

The impingement of a gas jet onto a surface results in a complex flow field. In the simplest case of jet discharging, a gas with a uniform initial velocity field of U_0 strikes a medium moving at zero velocity. The formation of the gas jets is illustrated in Figure 1. The short region of the jet in which the centerline velocity remains constant is called the initial region (Figure 1). The velocity profile reduces and expands with increasing the distance from the nozzle outlet. However, in the main region of the jet, the pressure is almost constant and equals the pressure in the ambiance (Khazaei et al., 2008a; Khazaei et al., 2008b). Following the turning of the jet in the impingement zone, the flow exits parallel with the surface (Figure 1).

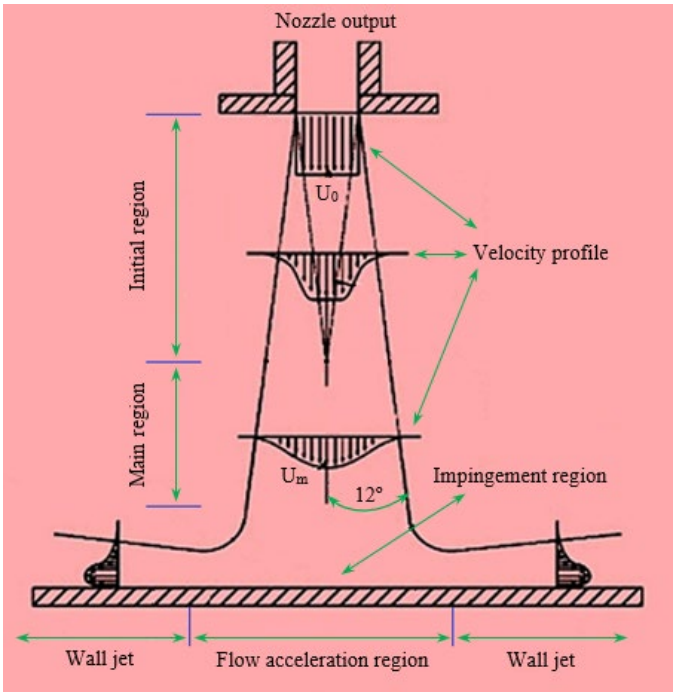

Figure 1 Formation of gas jet on a flat surface in three steps, 1) Exhaust gas from the nozzle with a square speed profile, 2) Deformation of a jet profile from square to bell, 3) The collision of gas jet to the horizontal surface and the gas exits Impingement region

When the jet temperature was equal to 20℃, the theoretical diameter of the initial covered region (DICR) and Initial Area of Covered Region (IACR) for different levels of nozzle diameter (at 4, 5, 6, 7 and 8 mm), and distance between the nozzle outlet and the surface of the

SH (at 10, 15, 20, 25 and 30 mm) were calculated.

Before carrying out the experiments, harvested flowers were classified into different categories based on the value of sunflower head diameter, and if the value of SH diameter ranged from 240 to 270 mm, it was used for the experimental tests. Mirzabe and Chegini (2015) measured the picking force of sunflower seeds for five different varieties (*Dorsefid, Mikhi, Shamshiri, Sirena,* and *Songhori*); they showed that for these varieties, sunflower head diameter has a significant effect on picking force. So, sunflower heads with diameters ranging from 240 to 270 mm were used to reduce the effect of the sunflower head diameter on the jet's performance. In order to examine the effect of air-jet parameters on the area of the removed region in different locations of the seed on SH, the selected SHs were divided into three regions, namely central region (CR), middle region (MR), and side region (SR), as shown in Figure 2.

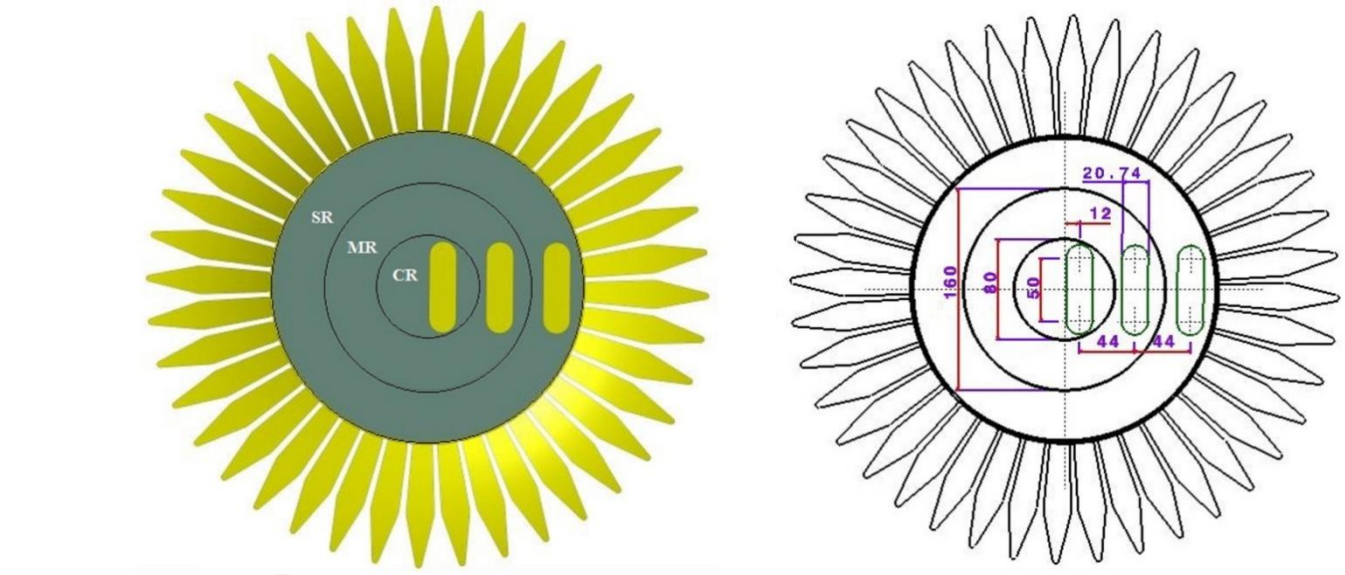

(A) **(B)**

Figure 2 (A) Three regions of SH. 1. Central region (CR) 2. Middle region (MR) 3. Side region (SR). (B) Three regions of SH and removing seeds in the regions using air-jet, in the critical case, when the SHD = 240 mm, NOD = 8 mm, DNS = 30 mm.

Mirzabe et al. (2012) measured sunflower seeds' dimensions and distance between adjacent seeds in different positions of seeds on a sunflower head. Also, Mirzabe and Chegini (2015) measured the picking force of sunflower seeds in different positions. Their work showed that, principally, each sunflower head could be divided into three regions with different properties. So, it was decided that the heads be divided into three regions. The diameter of each region (central region (CR), middle region (MR), or side region (SR)) was equal to 0.333 SHD (for example: if the sunflower head diameter was 270 mm, central region was an area between central point to diameter of 90 mm; middle region was an area between 90 to 180 mm; side region was an area between 180 to 270 mm.).

In each test, the whole area of the covered region by the air-jet should theoretically be in one of the CR, MR, or SR of the sunflower head. So, in cases in which the diameter of the sunflower head equals 240 mm, and the nozzle diameter equals 8 mm, the diameter of each region (CR, MR, or SR) equals 80 mm, and the diameter of the initial covered region by the nozzle equals to 20.74 mm. If the length of the linear movement of the sunflower head equals 50 mm and the distance between the nozzle center line and sunflower head center line in CR, MR, and SR equals 12, 56, and 100 mm, respectively, the whole area of the covered region by the air-jet would be theoretically

located in the one single intended region (see Figure 2. B.).

2.3 Experimental set-up

Figure 3 shows a schematic diagram of the experimental set-up used to evaluate the effects of operating parameters of the air-jet impingement on removing the sunflower seeds. This set-up works as follows: a rubber conveyer and an electro-motor were used to make the linear movement of the nozzle and sunflower head related to each other. The conveyor was made from Viton Rubber tires which are safe for food health. To change the linear velocity of the conveyors, the rotational velocity of the electro-motor was changed using an inverter (SV 015ic5-1F, LS industrial systems, China). The distance between the SHs and the nozzle outlet was set using a vertical guide shaft. A horizontal guide shaft was used to examine the effects of air-jet parameters on the area of the removed region in different locations of the seed on SH. The angle of impingement (angle between SH surface and air-jet) was set by changing the angle mechanisms (in the present study, the effect of angle of impingement was not examined). The pressure of the air increases in the piston compressor and the high-pressure flow of the air is transferred to the experimental set-up using pneumatic hoses. A switching valve is used to connect and disconnect the airflow.

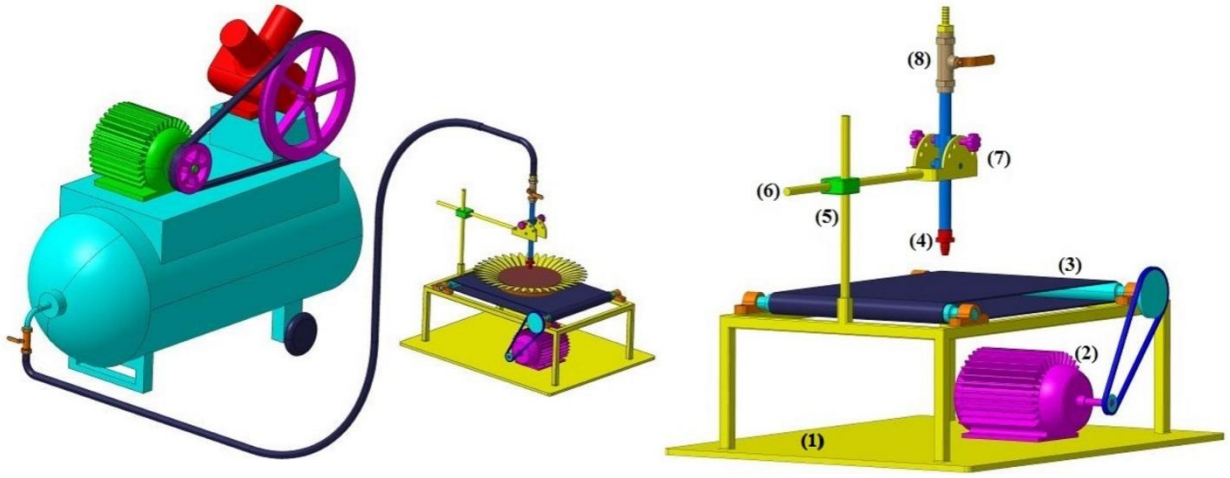

(1) frame, (2) electro-motor, (3) conveyor, (4) nozzle, (5) vertical guide shaft, (6) horizontal guide shaft, (7) changing angle mechanisms, (8) valve

Figure 3 Schematic of the experimental set-up used to evaluate the effects of operating parameters of the air-jet impingement on removing sunflower seeds.

Selection of electro-motor, chains, screws, and bearings was done based on engineering calculations and mentioned formulae in mechanical engineering books and handbooks (Pohanish and McCauley, 2000; Oberg et al., 1984; Shigley, 2011). All experiments were performed with three repetitions. The image processing technique was used to calculate the area of the removed regions.

2.4 Image processing set-up

The image processing system consisted of a camera (Canon, IXY 600F, Japan) with 3X IS lens capable of taking photos with a resolution of 12.1 megapixels, four white-colored fluorescent lamps (32 W), a USB connection, and a laptop computer (DELL, INSPIRON 1558, China) equipped with MATLAB R2012a software package. The camera was mounted on an image processing box (Mansouri et al., 2015; Mansouri et al., 2017). Each sunflower head was put at the center of the camera's field of view, three metal spheres with the same and identified diameters were put at the side of the sunflower head, and an RGB color image was taken from up view of the removed region of the sunflower head.

The original color image of each removed region and sphere was converted to an eight-bit gray-scale image. Eight-bit gray-scale intensity represents 256 different

shades of gray from black (0) to white (255). The eight-bit gray-scale images were digitized to a binary image using binary transformation based on all pixels with a brightness level which was the average of the brightness levels of the three channels (Uozumi et al., 1993). The threshold value of sunflower heads was determined experimentally (Koc, 2007). From the gray-scale image, pixel values less than 169 were converted to 0 (black), and the ones higher than 169 were converted to 255 (Koc, 2007; Mansouri et al., 2017). The threshold level of 169 was determined experimentally. The pixels with a value of 255 showed the removed regions of the head, and the ones with a value of 0 showed the remainder (Koc, 2007; Mansouri et al., 2017; Mansouri et al., 2015). Schematic representation of different steps of image processing is shown in Figure 4.

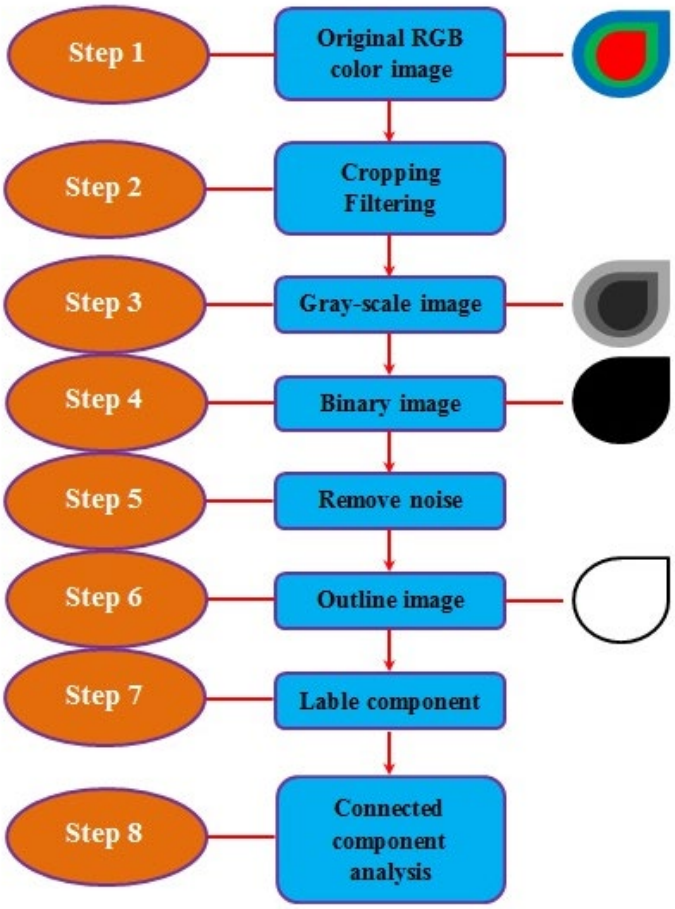

Figure 4 Schematic representation of different steps of image processing and original RGB color image, gray-scale image, binary image, and outline image for an imaginary object

2.5 Data analysis

For the *Shamshiri* variety, the effects of the linear velocity of the sunflower head (at 1, 2, and 3 cm sec^{-1}), nozzle diameter (at 4, 6, and 8 mm), the distance between the nozzle outlet and the surface of the SH (at 10, 20 and 30 mm), and reservoir pressure (at 600, 700 and 800 kPa) on the area of the removed region were studied. The MATLAB R2012a and Microsoft Excel Office 2010 software packages were used to analyze the taken photos and the data. Also, the maps of all parts of the machine were first designed in the CATIA V5R20 software package. All software packages were run on a DELL 1558 INSPIRON laptop computer.

3 Results and Discussions

3.1 Theoretical results

The calculated values of theoretical Diameter of Initial Covered Region (DICR), theoretical Initial and Final Areas of the Covered Region (IACR, FACR) for different levels of the nozzle diameter (at 4, 5, 6, 7, and 8 mm), and distance between nozzle outlet and sunflower head surface (at 10, 15, 20, 25 and 30 mm) are reported in Table 1. The data showed that DICR, IACR, and FACR increased as NOD and DNS increased from 4 to 8 mm and 10 to 30 mm, respectively.

Table 1 Effect of NOD and DNS on the theoretical diameter of the theoretical initial covered region (DICR), the initial area of the covered region (IACR), and final area of the covered region (FACR)

NOD (mm)	DNS (mm)	DICR (mm)	IACR (cm^2)	FACR (cm^2)
4	10	8.251	0.535	4.131
	15	10.377	0.846	5.197
	20	12.502	1.228	6.263
	25	14.628	1.680	7.331
	30	16.753	2.204	8.399
5	10	9.251	0.672	4.632
	15	11.377	1.016	5.698
	20	13.502	1.432	6.765
	25	15.628	1.918	7.833
	30	17.753	2.475	8.901
6	10	10.251	0.825	5.134
	15	12.377	1.203	6.200
	20	14.502	1.652	7.268
	25	16.628	2.171	8.335
	30	18.753	2.762	9.404
7	10	11.251	0.994	5.635
	15	13.377	1.405	6.702
	20	15.502	1.887	7.770
	25	17.628	2.440	8.838
	30	19.753	3.064	9.907
8	10	12.251	1.179	6.137
	15	14.377	1.623	7.204
	20	16.502	2.139	8.272
	25	18.628	2.725	9.341
	30	20.753	3.383	10.410

A comparison between the theoretical results showed an increase in DNS had a more significant effect on the increase in DICR, IACR, and FACR. Maximum values of DICR, IACR, and FACR were obtained when NOD and DNS were equal to 8 mm and 30 mm, respectively. Maximum values of DICR, IACR, and FACR were equal to 20.753 mm, 3.383 cm^2, and 10.410 cm^2, respectively. Minimum values of DICR, IACR, and FACR were obtained when ND and DNS were equal to 4 mm and 10 mm, respectively. Minimum values of DICR, IACR, and FACR were equal to 8.251 mm, 0.535 cm^2, and 4.131 cm^2, respectively.

In general, the relationship between DICR, IACR, and FACR to ND and DNS can be formulated in the following equations:

$$D_T = (D_N) + 2(D_{N-S})\,tan(12) = (D_N) + 0.4251(D_{N-S}) \quad (1)$$

$$A_{TI} = \frac{\pi}{100}\left\{\frac{[D_N+2(D_{N-S})\,tan(12)]^2}{4}\right\} = \frac{\pi}{400}\{(D_N)^2 + 0.1807(D_{N-S})^2 + 0.8502(D_N)(D_{N-S})\} \quad (2)$$

$$A_{TF} = \frac{\pi}{100}\left\{\frac{[(D_N)+2(D_{N-S})\,tan(12)]^2}{4}\right\} + 50\{(D_N) + 2(D_{N-S})\,tan(12)\} \quad (3)$$

3.2 Experimental results

3.2.1 Central region

The measured values of the removed region of the sunflower head for different levels of the linear velocity of SH, nozzle diameter, distance between nozzle outlet, sunflower head surface, and reservoir pressure are reported in Table 2. Data showed that the area of the removed region increased with increasing NOD, DNS, and PCR; also, the area of the removed region increased by decreasing linear velocity of SH.

A comparison between the experimental results in CR showed that increasing DNS had a more significant effect on increasing ARR, but a decrease in LVS had a lower effect on ARR. The maximum value of ARR in CR was obtained when LVS, NOD, DNS, and PCR were equal to 1 cm sec^{-1}, 8 mm, 30 mm, and 800 kPa, respectively. The minimum value of ARR in CR was obtained when LVS, NOD, DNS, and P were equal to 2 cm sec^{-1}, 4 mm, 10 mm, and 600 kPa, respectively. The maximum and minimum

values of ARR in the CR were equal to 10.608 and 2.247 cm^2, respectively.

The effects of the linear velocity of SH, nozzle diameter, the distance between nozzle outlet, and sunflower head surface, and reservoir pressure on the ratio of ARR to FACR (100ARR / FACR) in CR are reported in Table 3. The results showed that in all cases, the ratio of ARR to FACR increased with increasing reservoir pressure, while there is no particular trend for the other parameters.

Table 2 Effect of PCR, DNS, NOD and LVS on ARR in the central region (CR)

LVS (cm sec^{-1})	NOD (mm)	DNS (mm)	Area of the removed region, cm^2		
			Reservoir pressure (kPa)		
			600	700	800
1	4	10	2.707	3.191	3.752
		20	4.385	5.405	6.126
		30	6.287	7.231	9.032
	6	10	3.497	4.461	4.892
		20	5.291	5.783	7.886
		30	7.184	8.392	9.124
	8	10	4.281	5.953	6.016
		20	6.141	7.223	8.476
		30	8.078	9.544	10.608
2	4	10	2.462	2.906	3.532
		20	4.068	4.884	5.600
		30	5.297	6.961	8.482
	6	10	2.524	3.122	4.164
		20	4.272	5.670	6.792
		30	6.528	7.704	8.808
	8	10	3.952	4.686	5.572
		20	5.640	6.636	8.092
		30	7.505	8.188	10.536
3	4	10	2.247	2.693	3.236
		20	3.755	4.173	5.480
		30	5.621	6.273	7.956
	6	10	2.831	3.594	4.016
		20	4.313	5.009	6.048
		30	5.972	7.036	8.092
	8	10	3.523	4.299	4.828
		20	5.003	5.700	6.708
		30	6.774	7.984	9.180

The maximum value of the ratio of ARR to FACR in CR was obtained when LV, NOD, DNS, and P were equal to 1 cm sec^{-1}, 6 mm, 20 mm, and 800 kPa, respectively. The minimum value of the ratio of ARR to FACR in CR was obtained when LVS, NOD, DNS, and PCR were equal to 2 cm sec^{-1}, 6 mm, 10 mm, and 600 kPa, respectively. Maximum and minimum values of the ratio of ARR to FACR in CR were equal to 88.580% and 42.414%, respectively.

Table 3 Effect of PCR, DNS, NOD, and LVS on the ratio of removing sunflower seeds from their head (ARR) to the final area of the covered region (FACR) in the central region (CR)

LVS (cm sec^{-1})	NOD (mm)	DNS (mm)	100ARR / FACR (%)		
			Reservoir pressure (kPa)		
			600	700	800
1	4	10	58.088	68.474	80.512
		20	58.634	72.273	81.914
		30	59.419	68.341	85.362
	6	10	58.765	74.965	82.207
		20	59.431	64.958	88.580
		30	59.184	69.136	75.166
	8	10	58.610	81.501	82.363
		20	59.107	69.521	81.581
		30	58.711	69.365	77.099
2	4	10	52.831	62.358	75.791
		20	54.396	65.307	74.881
		30	50.063	65.789	80.164
	6	10	42.414	52.464	69.974
		20	47.985	63.688	76.291
		30	53.779	63.468	72.563
	8	10	54.106	64.154	76.284
		20	54.285	63.871	77.885
		30	54.546	59.510	76.575
3	4	10	48.217	57.788	69.439
		20	50.210	55.800	73.276
		30	53.125	59.287	75.193
	6	10	47.573	60.395	67.487
		20	48.446	56.264	67.934
		30	49.199	57.964	66.664
	8	10	48.232	58.856	66.099
		20	48.153	54.862	64.564
		30	49.233	58.027	66.720

3.2.2 Middle region

The measured values of the area of the removed region of sunflower head in MR for different levels of the linear velocity of SH, nozzle diameter, the distance between nozzle outlet and sunflower head surface, and also reservoir pressure are reported in Table 4. The data showed that ARR increased by increasing NOD, DNS, and PCR; also, the area of the removed region increased by decreasing the linear velocity of SH.

Table 4 Effect of PCR, DNS, NOD and LVS on ARR in the middle region (MR)

LVS (cm sec^{-1})	NOD (mm)	DNS (mm)	Area of the removed region, cm^2		
			Reservoir pressure (kPa)		
			600	700	800
1	4	10	4.751	5.057	5.312
		20	7.705	8.435	8.626
		30	10.891	11.337	12.792
	6	10	6.121	6.547	6.852
		20	9.163	9.441	10.266
		30	12.512	13.784	14.044
	8	10	7.533	8.031	8.496
		20	10.713	11.461	11.856
		30	14.154	15.148	15.248
2	4	10	4.366	4.662	4.992
		20	7.124	7.668	7.888
		30	10.321	11.047	11.952
	6	10	5.132	5.494	5.784
		20	8.496	9.090	9.552
		30	11.504	12.308	12.448
	8	10	6.936	7.422	7.832
		20	9.896	10.572	11.352
		30	13.168	14.076	14.816
3	4	10	3.943	4.211	4.616
		20	6.515	6.971	7.680
		30	9.953	10.671	11.136
	6	10	5.083	5.438	5.696
		20	7.609	8.143	8.508
		30	10.396	11.172	11.352
	8	10	6.239	6.673	6.768
		20	8.879	9.053	9.448
		30	11.782	12.674	13.580

A comparison between the experimental results in MR showed that increasing DNS had the most significant effect on increasing ARR while decreasing in LVS had the lowest effect on the increase in ARR. The maximum value of ARR in MR was obtained when the LVS, NOD, DNS, and PCR were equal to 1 cm sec^{-1}, 8 mm, 30 mm, and 800 kPa, respectively. The minimum value of ARR in MR was obtained when LVS, NOD, DNS, and PCR were equal to 3 cm sec^{-1}, 4 mm, 10 mm, and 600 kPa, respectively. Maximum and minimum values of ARR in MR were equal to 15.248 and 3.943 cm^2, respectively.

Table 5 Effect of PCR, DNS, NOD, and LVS on the ratio of removing sunflower seeds from their head (RSS) to the final area of the covered region (FACR) in the middle region (MR)

LVS (cm sec^{-1})	NOD (mm)	DNS (mm)	100ARR / FACR (%)		
			Reservoir pressure (kPa)		
			600	700	800
1	4	10	101.949	108.515	113.987
		20	103.028	112.789	115.343
		30	102.932	107.147	120.899
	6	10	102.860	110.019	115.144
		20	102.924	106.046	115.313
		30	103.077	113.556	115.698
	8	10	103.132	109.950	116.316
		20	103.112	110.311	114.113
		30	102.871	110.095	110.822
2	4	10	93.687	100.039	107.120
		20	95.259	102.533	105.475
		30	97.545	104.406	112.960
	6	10	86.241	92.324	97.197
		20	95.432	102.104	107.293
		30	94.773	101.397	102.550
	8	10	94.958	101.612	107.225
		20	95.248	101.755	109.262
		30	95.705	102.304	107.682
3	4	10	84.611	90.361	99.052
		20	87.116	93.213	102.694
		30	94.067	100.853	105.248
	6	10	85.417	91.383	95.718
		20	85.468	91.467	95.566
		30	85.645	92.038	93.521
	8	10	85.416	91.358	92.658
		20	85.460	87.134	90.936
		30	85.631	92.114	98.699

The effects of the linear velocity of SH, nozzle diameter, the distance between nozzle outlet and sunflower head surface, and also reservoir pressure on the ratio of ARR to FACR (100ARR / FACR) in MR are reported in Table 5. The results showed that in all cases, the ratio of ARR to FACR increased by increasing reservoir pressure, while for the other parameters, there is no certain trend.

The maximum value of the ratio of ARR to FACR in CR was obtained when LVS, NOD, DNS, and PCR were equal to 1 cm sec^{-1}, 4 mm, 30 mm, and 800 kPa, respectively. The minimum value of the ratio of ARR to FACR in CR was obtained when LVS, NOD, DNS, and PCR were equal to 3 cm sec^{-1}, 4 mm, 10 mm, and 600 kPa, respectively. The maximum and minimum values of the ratio of ARR to FACR in CR were equal to 120.899% and 84.611%, respectively.

3.2.3 Side region

The measured values of the area of the removed region of sunflower head in the SR, for the different levels of the linear velocity of SH, nozzle diameter, the distance between nozzle outlet and sunflower head surface, and also reservoir pressure are reported in Table 6. The data showed that ARR increased with increasing NOD, DNS, and PCR; also, the area of the removed region increased with decreasing linear velocity of SH.

Table 6 Effect of PCR, DNS, NOD, and LVS on ARR in the side region (SR)

LVS (cm sec^{-1})	NOD (mm)	DNS (mm)	Area of the removed region, cm^2		
			Reservoir pressure (kPa)		
			600	700	800
1	4	10	5.159	5.385	5.896
		20	8.345	9.425	9.776
		30	11.119	12.755	13.920
	6	10	6.689	7.265	7.620
		20	9.967	11.015	11.160
		30	13.808	15.360	15.047
	8	10	8.297	9.145	9.441
		20	11.617	12.715	13.460
		30	15.486	16.897	16.998
2	4	10	4.794	5.113	5.524
		20	7.766	8.572	8.805
		30	11.249	11.405	13.392
	6	10	5.593	6.171	6.464
		20	9.264	10.050	10.632
		30	12.536	13.720	13.968
	8	10	7.564	8.248	8.722
		20	10.764	11.708	12.632
		30	14.312	16.044	16.660
3	4	10	4.287	4.465	5.505
		20	7.135	8.165	8.574
		30	10.877	11.165	12.676
	6	10	5.547	5.370	5.976
		20	8.281	9.245	9.328
		30	11.364	12.468	12.282
	8	10	6.510	7.495	7.648
		20	9.811	9.995	10.952
		30	12.238	14.151	15.466

A comparison between the experimental results in SR showed that an increase in DNS had greater effect on increase in ARR while decreasing LVS had the lowest effect on increasing ARR. The maximum value of ARR in SR was obtained when LVS, NOD, DNS, and PCR were equal to 1 cm sec^{-1}, 8 mm, 30 mm, and 800 kPa, respectively. The minimum value of ARR in MR was obtained when LVS, NOD, DNS, and PCR were equal to 3 cm sec^{-1}, 4 mm, 10 mm, and 600 kPa, respectively. The maximum and minimum values of ARR in the SR were equal to 16.998 and 4.287 cm^2, respectively.

The effects of the linear velocity of SH, nozzle diameter, the distance between nozzle outlet and sunflower head surface, and also reservoir pressure on the ratio of ARR to FACR (100ARR / FACR) in SR are reported in Table 7. The results showed that in most cases, the ratio of ARR to FACR increased by increasing reservoir pressure, while there is no certain trend for the other parameters.

The maximum value of the ratio of ARR to FACR in CR was obtained when LVS, NOD, DNS, and PCR were equal to 1 cm sec^{-1}, 4 mm, 30 mm, and 800 kPa, respectively. The minimum value of the ratio of ARR to FACR in CR was obtained when LVS, NOD, DNS, and P were equal to 3 cm sec^{-1}, 8 mm, 30 mm, and 600 kPa, respectively. The maximum and minimum values of the

ratio of ARR to FACR in CR were equal to 131.560% and 88.945%, respectively.

Table 7 Effect of PCR, DNS, NOD, and LVS on the ratio of removing sunflower seeds from their head (RSS) to the final area of the covered region (FACR) in the side region (SR)

LVS (cm sec^{-1})	NOD (mm)	DNS (mm)	100ARR / FACR (%)		
			Reservoir pressure (kPa)		
			600	700	800
1	4	10	110.704	115.554	126.519
		20	111.586	126.027	130.721
		30	105.087	120.549	131.560
	6	10	112.405	122.084	128.050
		20	111.955	123.726	125.355
		30	113.754	126.540	123.961
	8	10	113.591	125.201	129.254
		20	111.813	122.381	129.551
		30	112.552	122.807	123.541
2	4	10	102.872	109.717	118.536
		20	103.844	114.621	117.737
		30	106.316	107.790	126.569
	6	10	93.987	103.700	108.624
		20	104.058	112.887	119.424
		30	103.275	113.029	115.072
	8	10	103.556	112.921	119.410
		20	103.603	112.688	121.582
		30	104.019	116.607	121.084
3	4	10	91.992	95.812	118.129
		20	95.406	109.179	114.648
		30	102.800	105.522	119.802
	6	10	93.214	90.240	100.424
		20	93.017	103.845	104.777
		30	93.620	102.715	101.182
	8	10	89.126	102.612	104.706
		20	94.430	96.201	105.412
		30	88.945	102.849	112.406

3.3 Modeling and optimization

Modeling of ARR using independent parameters is needed for determining the interaction effects and predicting values of ARR when values of the independent parameters change. Linear and quadratic models were applied to model the ARR using independent parameters, including PCR, LVS, NOD, and DNS parameters. Linear and quadratic models of ARR in CR of a sunflower head are mentioned in the two following equations, respectively:

$$A_{RR}(CR) = 0.9796\,P - 0.5297\,V_L + 0.4387\,D_N + 0.199\,D_{N-S} - 6.6330, \quad R^2 = 0.9703 \tag{4}$$

$$A_{RR}(CR) = -0.6734\,P + 0.3045\,V_L - 0.133\,D_N - 0.1133\,D_{N-S} - 0.0710\,(P \times V_L) + 0.0382\,(P \times D_N) + 0.0294\,(P \times D_{N-S}) - 0.0783\,(V_L \times D_N) - 0.0009\,(V_L \times D_{N-S}) - 0.0002\,(D_N \times D_{N-S}) + 0.0608\,(P)^2 + 0.07637\,(V_L)^2 + 0.0410\,(D_N)^2 + 0.0008\,(D_{N-S})^2 + 1.8787, \quad R^2 = 0.9868 \tag{5}$$

As can be seen, the value of R-square (R^2) in the quadratic model was more than its value in the linear model. It means that the quadratic model's accuracy to predict ARR values is more than the linear model, but it must be considered that the quadratic model has more constant coefficients. However, it is apparent that differences between the values of ARR predicted by linear and quadratic models are significant, so it is better to use the quadratic model.

The linear and quadratic models of ARR in MR and SR of a sunflower head are mentioned in Equation 6 - Equation 9, respectively. The values of R-square (R^2) in the quadratic models were more than its values in the linear models, but the accuracy of linear models is acceptable, and the differences between accuracy of quadratic and linear models are not significant; therefore, in two cases (MR and SR), using linear models was more applicable than the quadratic models, because the predicted values of both models were not significantly different, but the application of the quadratic model has more complexities.

$$A_{RR}(MR) = 0.5186\,P - 0.7794\,V_L + 0.6776\,D_N + 0.3227\,D_{N-S} - 3.5014, \quad R^2 = 0.9866 \tag{6}$$

$$A_{RR}(MR) = 1.0719\,P + 0.7156\,V_L + 0.2427\,D_N + 0.1585\,D_{N-S} - 0.0434\,(P \times V_L) + 0.0093\,(P \times D_N) + 0.0179\,(P \times D_{N-S}) - 0.1157\,(V_L \times D_N) - 0.0199\,(V_L \times D_{N-S}) + 0.0007\,(D_N \times D_{N-S}) - 0.0629\,(P)^2 - 0.0246\,(V_L)^2 + 0.0489\,(D_N)^2 + 0.0019\,(D_{N-S})^2 + 4.1819, \quad R^2 = 0.9949 \tag{7}$$

$$A_{RR}(SR) = 0.7064\,P - 0.8665\,V_L + 0.7752\,D_N + 0.3546\,D_{N-S} - 4.9249, \quad R^2 = 0.9810 \tag{8}$$

$$A_{RR}(SR) = 1.0719\,P + 0.7156\,V_L + 0.2427\,D_N + 0.1585\,D_{N-S} - 0.0132\,(P \times V_L) + 0.0284\,(P \times D_N) + 0.0252\,(P \times D_{N-S}) - 0.1508\,(V_L \times D_N) - 0.0184\,(V_L \times D_{N-S}) + 0.0038\,(D_N \times D_{N-S}) - 0.1504\,(P)^2 - 0.0482\,(V_L)^2 + 0.0641\,(D_N)^2 + 0.0009\,(D_{N-S})^2 - 7.4660 \quad , R^2 = 0.9910 \quad (9)$$

Table 8 Response surface method (RSM) optimization of ARR in CR, MR, and SR

Region	Parameter	Weight of parameter	Range of parameter	Points		
				Point 1	Point 2	Point 3
Central region (CR)	PCR, bar	2	6 – 8	7.38	7.07	6.89
	LVS, cm sec^{-1}	2	1 – 3	1.47	2.54	2.74
	NOD, mm	4	4 – 8	5.13	5.13	5.13
	DNS, mm	1	10 – 30	24.93	24.93	24.93
	ARR, cm^2	-	2.247 – 10.608	6.948	5.993	5.732
Middle region (MR)	PCR, bar	2	6 – 8	6.41	6.30	6.93
	LVS, cm sec^{-1}	2	1 – 3	1.96	1.98	2.63
	NOD, mm	4	4 – 8	5.13	5.13	5.13
	DNS, mm	1	10 – 30	24.93	24.93	24.93
	ARR, cm^2	-	3.943 – 15.248	9.630	9.542	9.436
Side region (SR)	PCR, bar	2	6 – 8	6.59	7.00	6.66
	LVS, cm sec^{-1}	2	1 – 3	2.05	2.51	2.31
	NOD, mm	4	4 – 8	5.13	5.13	5.13
	DNS, mm	1	10 – 30	24.93	24.93	24.93
	ARR, cm^2	-	4.287 – 16.998	10.664	10.626	10.506

When the PCR, LVS, NOD, and DNS become double, the mass flow rate of nozzle or energy consumption becomes double, halve, fourfold and unchanged; therefore, the weight of parameter of P, LVS, NOD, and DNS was considered as 2, 2, 4 and 1, respectively.

Optimization provides an elegant blend of theory and application. Optimization allows users to get the most out of a given system. In a way, it is the minimization of waste. Optimization can often shed new light in design when considering the coupling of multiple systems; therefore, response surface method (RSM) optimization was performed to determine the interaction effects of PCR, LVS, NOD, and DNS parameters. Data were analyzed using the response surface regression procedure and fitted to the second-order quadratic equation. The Design Expert 8 software package was used to analyze the data.

The ARR, PCR, NOD, and time of the test (LVS) were considered as responses of the test; because the purpose was to design and construct a machine for removing sunflower seeds from the SH with the lowest power and energy consumption. It should be noted that when the nozzle diameter and pressure increase, mass flow rate, power, and energy consumption increase, too; also with increasing time (decreasing LVS) of the test, with a constant value of power consumption, energy consumption increases, too; therefore, optimum conditions for removing seeds from the SH were obtained when the ARR, PCR, NOD, and LVS of the test were maximum, minimum, and minimum, respectively. The interaction effects of PCR, LVS, NOD, and DNS on machine performance for CR, MR, and SR are shown in Table 8.

Three optimal points of each region of the sunflower head are shown in Table 8. According to RSM optimization results, one of the optimal conditions of machine operation in CR belonged to P of 7.38 bar, LVS of 1.47 cm sec^{-1}, NOD of 5.13 mm, and DNS of 24.93 mm. In this case, ARR is equal to 6.948 cm^2. One of the optimal machine operation conditions in MR belonged to P of 6.41 bar, LVS of 1.96 cm sec^{-1}, NOD of 5.13 mm, and DNS of 24.93 mm. In this case, ARR is equal to 9.630 cm^2. The corresponding SR values are 6.59 bar, 2.05 cm sec^{-1}, 5.13 mm, 24.93 mm, and 10.664 cm^2.

3.4 Power consumption analysis

Power consumption of the machine (without considering compressor) was calculated to be less than

0.100 kW (power consumption of electro-motor) for different ranges of operational parameters. For the optimization to be carried out appropriately, the amount of power consumption of the compressor must be calculated. At the first step, the mass flow rate of nozzles and compressor efficiency must be known. The critical mass flow rate for a perfect gas with constant specific heat is determined by Equation 10 (Fay and Sonwalkar, 1996):

$$\dot{m} = \rho_s \; V_{ls} \, A \left(\frac{2}{k+1}\right)^{\frac{k+1}{2(k-1)}} \quad (10)$$

Where: ρ_s is the density of supply air; A is the nozzle exit area; k is specific heat transfer *(*the ratio of the heat capacity at constant pressure to the heat capacity at constant volume), and V_{ls} is the local speed of sound.

In the next step, piston compressor efficiency must be calculated; so, the following equation was used (Dixon and Hall, 2013; Ueno et al., 2003):

$$\eta_C = 0.97 - C \left\{\left(\frac{Z_1}{Z_2}\right)\left(\frac{P_2}{P_1}\right)^{\frac{1}{\gamma}} - 1\right\} - L \quad (11)$$

Where: η_C (dimensionless) is volumetric flow efficiency of the compressor, Z_1 and Z_2 (dimensionless) are compressibility factors of air in input and output of the compressor, P_1 and P_2 (in Pa or bar) are air pressures in input and output of the compressor, L is lubrication factor (L ranges between 0.05 and 0.06 for lubricated compressors and ranges between 0.09 and 0.1 for non-lubricated compressors), C is the percentage of dead space (C ranges between 0.06 and 0.12).

In the last step, the power consumption of the piston compressor was calculated based on the following equation (Bejan, 2016; Ueno et al., 2003):

$$P_C = \left(\frac{R \,.\, Z \,.\, \dot{m}}{\eta_M \,.\, \eta_P}\right)\left(\frac{\gamma}{\gamma-1}\right)\left\{\left(\frac{P_2}{P_1}\right)^{\left(\frac{\gamma}{\gamma-1}\right)} - 1\right\} \quad (12)$$

Where: P_C is power consumption in kW, η_M is mechanical efficiency, Z is compressibility factor, $\dot{m}$ is the mass flow rate in kg sec^{-1}, R is the real gas constant (R= 8.314 J K^{-1} mol^{-1}), γ is specific heat transfer of polytrophic process that ranges from 1.30 to 1.35, and P_1 and P_2 are air pressures in input and output of the compressor, and η_P is polytrophic efficiency that can be calculated as:

$$\eta_P = \frac{\gamma\,(k-1)}{k\,(\gamma-1)} \quad (13)$$

Based on the mentioned equations, power and energy consumption of the compressor was calculated for each test condition (Table 9).

Table 9 Calculation of power and energy consumption of air compressor for each test

PCR (kPa)	NOD (mm)	LVS (cm sec^{-1})	Mass flow rate (cm sec^{-1})	Compressor's power (kW)	Energy consumption for each test (W h)
600	4	1	0.017536877	0.2533	0.3519
		2			0.1759
		3			0.1173
	6	1	0.039457973	0.5697	0.7912
		2			0.3956
		3			0.2637
	8	1	0.070147507	1.0127	1.4065
		2			0.7032
		3			0.4688
700	4	1	0.020465534	0.3683	0.5116
		2			0.2558
		3			0.1705
	6	1	0.046047451	0.8290	1.1514
		2			0.5757
		3			0.3838
	8	1	0.081862136	1.4737	2.0468
		2			1.0234
		3			0.6823
800	4	1	0.023395865	0.5043	0.7005
		2			0.3502
		3			0.2335
	6	1	0.052640696	1.1347	1.5759
		2			0.7880
		3			0.5253
	8	1	0.093583459	2.0173	2.8019
		2			1.4009
		3			0.9340

Based on the compressor's model, constant coefficients were considered to be P_1 = 1 bar, C = 0.090, L = 0.050, γ = 1.300, η_M = 0.90, and η_P = 1.2381 which were obtained when the NOD, LVS, DNS, and PCR were equal to 5 mm,

3.099 cm sec^{-1}, 18.221 mm, and 7.438 bar, respectively (optimized values of operational parameters).

As can be seen, in Table 9 (also, as mentioned before), an increase in the pressure and nozzle diameter causes an increase in the mass flow rate, which causes an increase in power and energy consumption. Also, a decrease in linear velocity causes increase in the test time, which causes increased energy consumption (without changing in power consumption). Based on calculations, the minimum and maximum energy consumption values were 0.1173 and 2.8019 W h, respectively.

Mass flow rate, power, and energy consumption were calculated for optimized points in the three regions of SH (Table 10). The maximum and minimum values of mass flow rate were 0.035457565 (point 1 in CR) and 0.030275627 (point 2 in MR) kg sec^{-1}, respectively. Like mass flow rate, the maximum and minimum of power consumption occurred in point 1 in CR and point 2 in MR, and their values were 0.686 and 0.470 kW. Like mass flow rate and power consumption, the maximum energy consumption occurred in point 1 in CR, and its value was 0.6486 W h; while the minimum value of energy consumption occurred in point 3 in CR and its value was 0.2957 W h.

Table 10 Calculation of mass flow rate, power consumption, and energy consumption of air compressor for optimized points in three regions

Region	Optimized points	Mass flow rate (cm sec^{-1})	Compressor's power (kW)	Energy consumption (W h)
CR	Point 1	0.035457565	0.686	0.6486
	Point 2	0.033975981	0.620	0.3392
	Point 3	0.033118593	0.583	0.2957
MR	Point 1	0.030797154	0.490	0.3472
	Point 2	0.030275627	0.470	0.3294
	Point 3	0.033310863	0.591	0.3123
SR	Point 1	0.031661972	0.524	0.3550
	Point 2	0.033639585	0.606	0.3352
	Point 3	0.032013037	0.538	0.3232

4 Discussions

4.1 Theoretical discussions

By increasing the nozzle diameter or distance from the nozzle outlet, the cross-section of the air-jet increases because the air-jets were expanded as a frustum (see Figure 1). Therefore, when the nozzle diameter or distance between the nozzle outlet and the surface of the SH increases, the diameter of the initial covered region (DICR), the initial area of the covered region (IACR), and the final area of the covered region (FACR) by air-jet will increase.

4.2 Experimental discussions

Experimental results indicated that in the identical conditions (identical linear velocity of SH, identical pressure, identical nozzle diameter, identical angle of impingement, and identical distance between the nozzle outlet and the surface of the SH), the areas of the removed region in side and central regions were the highest and lowest, respectively. Since for each head, the seeds located on the side region of the head reach maturity before the seeds located on the middle region of the head (Mirzabe and Chegini, 2015). Also, seeds located on the middle region of the head reach maturity before the seeds located on the central region of the head.

The physiological maturity of sunflower heads starts from the side region to the central one. So when the sunflower head matures, there are immature seeds in the central region that are still absorbing nutrition from the plant. Therefore, in most cases in the central region, maturity does not happen ultimately, and so picking force of the seeds in the central region is more than the side and middle regions, and the value of picking force on the middle region is more than the side one (Mirzabe et al., 2014; Mirzabe and Chegini, 2015).

4.3 Comparison between experimental and theoretical results

Based on the theoretical results, with increasing nozzle diameter and reservoir pressure, mass flow rate, jet momentum, jet force, and area of the removed region will increase; the experimental results confirmed the theoretical ones.

Based on the theoretical results, with an increase in distance between the nozzle outlet and the surface of the

SH, the area of the covered region increases; the experimental results showed that with an increase in distance between the nozzle outlet and the surface of the SH, the area of the removed region increases. When the distance of the nozzle outlet from the head surface increases, the area of the covered region by air-jet increases, while jet force decreases. Therefore, it cannot be said that the area of the removed region increases by an increasing distance of the nozzle outlet from the head because the jet force decreases, and after a certain point, the air-jet force loses its ability to remove the seeds.

Results showed that in all three regions, with an increasing linear velocity of SH, the area of the removed region by air-jet decreases. Based on the theory, with an increasing linear velocity of SH, the focus of the jet on the covered region by the jet decreases, and the area of the removed region by air-jet will decrease. Also, results showed that in all three regions, with increasing reservoir pressure, the area of the removed region increases by air-jet. Based on the theory, increasing reservoir pressure will result in mass flow rate, jet momentum, and jet force increment. Therefore, the area of the removed region by air-jet will increase.

Comparison between experimental results and theoretical calculations showed that for SR in 69 cases out of 81, and for MR in 46 cases out of 81, the values of the area of the removed region were more than the area of the theoretical covered region by air-jet. In contrast, in CR, in all cases, the values of the area of the removed region were less than the area of the theoretical covered region by air-jet. It means that in removing sunflower seeds from SH in SR and MR, in addition to vertical flows impinged to SH surface, the horizontal flow exits parallel to the surface, resulting in removing seeds from SH. In CR, the picking force of sunflower seeds is more than the picking force in SR and MR (Mirzabe and Chegini, 2015). Therefore, the horizontal flow exits parallel to the surface cannot remove the seeds from SH.

The practical results showed that, in all three regions, in most cases, the ratio of ARR to FACR increased with increasing reservoir pressure, while for the other parameters, there is no particular trend. Theoretically, with increasing reservoir pressure, mass flow rate and jet force increase; consequently, ARR increases, while FACR does not change, and it means that the ratio of ARR to FACR will increase with increasing reservoir pressure. Based on the theory, with increasing nozzle diameter, both ARR and FACR increase. Experimental results did not show any relations between increasing nozzle diameter and the ratio of ARR to FACR. Also, based on the theory, with increasing DNS, FACR increases, and ARR can increase or decrease (increasing or decreasing of ARR depends on the value of the DBS). So, based on the theory, there is no descending or increment function that can produce a relation between DNS and the ratio of ARR to FACR. Also, experimental results did not show any certain trend.

Effects of the seed's location, angle of impingement, the distance between nozzle and sunflower head surface, and rotational velocity of sunflower head on the percentage of extracted seeds were studied by Mirzabe et al. (2014). Their results showed that, in rotational movement, with increasing nozzle diameter and nozzle pressure, the percentage of extracted seeds increases; in the current study, the same trends for nozzle diameter and pressure were observed. Also, Mirzabe et al. (2014) mentioned that with increasing DNS from 10 to 20 mm and decreasing DNS from 40 to 20 mm, the percentage of extracted seeds increases; the same results were observed in the current study; results showed that with increasing DNS from 10 to 20 mm and decreasing DNS from 30 to 20 mm, area of the removed region increased.

Mirzabe et al. (2014) mentioned that, in rotational movement, with increasing rotational velocity from 10 to 30 rev min^{-1}, the percentage of extracted seeds increases; also, in the current study, the same trend was observed for linear velocity; with increasing linear velocity from 1 to 3 cm sec^{-1}, area of the removed region increased. Decreasing the percentage of the removed seeds or removed area because of increasing linear or rotational velocity can be explained by the theory. Based on the theory of the jets,

with increasing linear or rotational velocity, the focus of the jet (or jets) on the covered region decreases, and the percentage of the removed seeds or removed area decreases.

5 Conclusions

The final aim of the authors was to design and construct an air jet impingement-based sunflower thresher machine. Based on the conducted investigations and literature review, in the design of that machine, to successfully remove seeds from sunflower heads, a mix of rotational movement of nozzles and linear movement of sunflower head is needed. In the previous studies, performances of effective parameters of prototype machine in the rotational movement were investigated. In the current study, the effects of parameters were considered in the linear movement of sunflower heads. The obtained results from the present study will help researchers to design the final thresher machine.

The effects of some of the most critical parameters of air-jet impingement on removing sunflower seeds from their heads were examined when the sunflower head had linear velocity, and the nozzle was fixed. Also, theoretical values of the area of the covered region by air-jet impingement for different levels of distances between the nozzle outlet and the surface of SH and nozzle diameters were calculated. Also, the theoretical covered region and the area of the removed region were compared together.

Results showed that in the side region, in 69 cases out of 81, and in the middle region, in 46 cases out of 81, the values of the area of the removed region were more than the area of the theoretical covered region by air-jet;. In contrast, in the central region, in all cases, the values of the area of the removed region were less than the area of the theoretical covered region by air-jet.

In all tests, no seeds were observed to have been damaged due to air-jet impingement. The maximum and minimum values of ARR in SR were equal to 16.998 and 4.287 cm^2, respectively. The maximum and minimum values of ARR in MR were equal to 15.248 and 3.943 cm^2, respectively; the corresponding values in CR were equal to 10.608 and 2.247 cm^2, respectively.

Experimental data were modeled using linear and quadratic functions and optimized based on RSM. Modeling results showed that linear and quadratic functions had a good performance and an acceptable accuracy in all cases. Optimizing results showed that, in optimal conditions, the values of ARR were equal to 6.948, 9.630, and 10.664 cm^2 in CR, MR, and SR, respectively.

Acknowledgments

The authors would like to thank the University of Tehran for providing technical support for this work. We would also like to sincerely thank Mr. Asghar Mirzabe, Mr. Mahdi Malati, Eng. Ali Javadi and Eng. Javad Yousefi, Dr. Ali Fadavi, Prof. Mohammad Hossein Kianmehr for their technical help and supervision while writing the paper. We would also like to thank Mr. Mohammad Hassan Torabi for his valuable support in editing the text of the paper.

References

Ando, T., T. Suzuki, K. Ishii, H. Omura, and J. Yamazaki. 1988. Apparatus for separating juice sacs of citrus fruits. U.S. Patent 4,738,194 (In U. S.).

Anil, J., T. Guruswamy, S. R. Desai, T. Basavaraj, and A. Joshi. 1998. Effect of cylinder speed and feed rate on the performance of thresher. *Journal of Agricultural Sciences*, 4(1): 120–21.

Bansal, N. K., and B. S. Dahiya. 2001. Effect of threshing techniques on quality of sunflower seed. *Seed Research-New Delhi-,* 29(1): 52–57.

Bejan, Adrian. 2016. Advanced Engineering Thermodynamics. USA. John Wiley & Sons, Inc.

Darvishzadeh, R., A. Pirzad, H. Hatami-Maleki, S. Poormohammad-Kiani, and A. Sarrafi. 2010. Evaluation of the reaction of sunflower inbred lines and their f1 hybrids to drought conditions using various stress tolerance indices. *Spanish Journal of Agricultural Research*, 8(4): 1037–46.

Dixon, S. L., and C. Hall. 2013. Fluid Mechanics and Thermodynamics of Turbomachinery. Oxford, England. Butterworth-Heinemann.

Fay, J. A., and N. Sonwalkar. 1996. A Fluid Mechanics Hypercourse. Cambridge, Massachusetts, USA: The MIT Press.

Gardon, R., and J. C. Akfirat. 1966. Heat transfer characteristics of impinging two-dimensional air jets. *Journal of Heat Transfer*, 88(1): 101–107.

Goel, A. K., D. Behera, S. Swain, and B. K. Behera. 2009. Performance evaluation of a low-cost manual sunflower thresher. *Indian Journal of Agricultural Research*, 43(1): 37–41.

Goldstein, R. J., A. I. Behbahani, and K. K. Heppelmann. 1986. Streamwise distribution of the recovery factor and the local heat transfer coefficient to an impinging circular air jet. *International Journal of Heat and Mass Transfer,* 29(8): 1227–1235.

Hayashi, M., Y. Ifuku, H. Uchiyama, Y. Kaga, and A. Nakamori. 1981. Apparatus for extracting pulp from citrus fruits. U.S. Patent 4,300,448 (In U. S.).

Huang, L., and M. S. El-Genk. 1994. Heat transfer of an impinging jet on a flat surface. *International Journal of Heat and Mass Transfer*, 37(13): 1915–1923.

Khazaei, J., N. Ekrami-Rad, M. Safa, and S. Z. Nosrati. 2008a. Effect of air-jet impingement parameters on the extraction of pomegranate arils. *Biosystems Engineering*, 100(2): 214–226.

Khazaei, J., J. Massah, and G. H. Mansouri. 2008b. Effect of some parameters of air-jet on pneumatic extraction of citrus juice and juice sacs. *Journal of Food Engineering*, 88(3): 388–398.

Koc, A. B. 2007. Determination of watermelon volume using ellipsoid approximation and image processing. *Postharvest Biology and Technology*, 45(3): 366–371.

Mansouri, A., A. Fadavi, and S. M. M. Mortazavian. 2015. Effects of length and position of hypocotyl explants on Cuminum Cyminum L. callogensis by image processing analysis. *Plant Cell, Tissue and Organ Culture (PCTOC)*, 121(3): 657–666.

Mansouri, A., A. H. Mirzabe, and A. Ráufi. 2017. Physical properties and mathematical modeling of melon (Cucumis Melo L.) seeds and kernels. *Journal of the Saudi Society of Agricultural Sciences*, 16(3): 218-226.

Martin, H. 1977. Heat and mass transfer between impinging gas jets and solid surfaces. In *Advances in Heat Transfer*, 13(1): 1–60.

Mirzabe, A. H., and G. R. Chegini. 2016. Effect of air-jet impingement parameters on the removing of sunflower seeds from the heads in static conditions. *Agricultural Engineering International: CIGR Journal*, 18(2): 43-59.

Mirzabe, A. H., and G. R. Chegini. 2015. Measuring picking force of sunflower seeds and prediction of reasonable range of air-jet parameters to remove sunflower seeds from the head. *Agricultural Engineering International: CIGR Journal*, 17(3): 415-429.

Mirzabe, A. H., G. R. Chegini, J. Khazaei, and J. Massah. 2014. Design, Construction and evaluation of preliminarily machine for removing sunflower seeds from the head using air-jet impingement. *Agricultural Engineering International: CIGR Journal*, 16(1): 294–302.

Mirzabe, A. H., J. Khazaei, and G. R. Chegini. 2012. Physical properties and modeling for sunflower seeds. *Agricultural Engineering International: CIGR Journal*, 14(3): 190–202.

Nahir, D., and B. Ronen. 1992. Apparatus for removing pulp from fruit. U.S. Patent 5178057 (In U. S.).

Nderitu, J., G. Nyamasyo, M. Kasina, and M. L. Oronje. 2008. Diversity of sunflower pollinators and their effect on seed yield in makueni district, eastern kenya. *Spanish Journal of Agricultural Research*, 6(2): 271–278.

Oberg, E., F. D. Jones, and H. L. Horton. 1984. Machinery's Handbook. New York, USA. HH Ryffel, ed.

Pohanish, R. P., and C. J. McCauley. 2000. *Machinery's Handbook Pocket Companion*. New York, USA. Industrial Press Inc.

Polat, S. 1993. Heat and mass transfer in impingement drying. *Drying Technology*, 11(6): 1147–1176.

Razi, H., and M. T. Assad. 1998. Evaluating Variability of important agronomic traits and drought tolerant criteria in sunflower cultivars. *Isfahan University of Technology-Journal of Crop Production and Processing*, 2(1): 31–44.

Rodi, W. 2014. Turbulent Buoyant Jets and Plumes: HMT: The Science & Applications of Heat and Mass Transfer. Reports, Reviews & Computer Programs. Germany. Elsevier.

Sarig, Y., Y. Regev, and F. Grosz. 1985. Apparatus for separating pomegranate seeds, scanning apparatus and techniques useful in connection therewith and storage and packaging techniques for separated seeds. U.S. Patent 4530278 (In U. S.).

Schmilovitch, Z., Y. Sarig, A. Daskal, E. Weinberg, F. Grosz, B. Ronen, A. Hoffman, and H. Egozi. 2014. Apparatus and method for extracting pomegranate seeds from pomegranates. U.S. Patent 7968136 (In U. S.).

Sharma, K. D., and R. S. Devnani. 1979. Threshing studies on sunflower thresher. *Agricultural Mechanization in Asia, Africa and Latin America*, 10(2): 69–72.

Shigley, J. E. 2011. Shigley's Mechanical Engineering Design. New York, USA. Tata McGraw-Hill Education.

Sudajan, S., V. M. Salokhe, and S. Chusilp. 2005. Effect of concave hole size, concave clearance and drum speed on rasp-bar drum performance for threshing sunflower. *Agricultural Mechanization in Asia Africa And Latin America*, 36(1): 52.

Sudajan, S., V. M. Salokhe, S. Chusilp, and V. Plermkamon. 2003. Power requirement and performance factors of a sunflower

thresher. *Agricultural Science. Journal*, 34(4): 205-208.

Ueno, K., R. E. Bye, and K. S. Hunter. 2003. Compressor Efficiency Definitions. *University of Colorado.*

Uozumi, N., T. Yoshino, S. Shiotani, K.I. Suehara, F. Arai, T. Fukuda, and T. Kobayashi. 1993. Application of image analysis with neural network for plant somatic embryo culture. *Journal of Fermentation and Bioengineering*, 76(6): 505–509.

Viskanta, R. 1993. Heat transfer to impinging isothermal gas and flame jets. *Experimental Thermal and Fluid Science*, 6(2): 111–134.

Webb, B. W., and C. F. Ma. 1995. Single-phase liquid jet impingement heat transfer. In *Advances in Heat Transfer*, 26(1): 105–217. Elsevier.

Yeranee, K., M. Wae-hayee, I. Piya, Y. Rao, and C. Nuntadusit. 2017. The study of flow and heat transfer characteristics of impinging jet array mounting air-induced duct. In *IOP Conference Series: Materials Science and Engineering*, 243(1): 1-10.

Zuckerman, N., and N. Lior. 2006. Jet impingement heat transfer: physics, correlations, and numerical modeling. *Advances in Heat Transfer*, 39: 565–631.

Nomenclature

Symbol	Definition	Abbreviation	Unit
-	Central region of sunflower head	*CR*	-
-	Middle region of sunflower head	*MR*	-
-	Sunflower head	*SH*	-
-	Sunflower head diameter	*SHD*	mm
-	Sunflower heads	*SHs*	-
-	Side region of sunflower head	*SR*	-
A	Area of the nozzle exit,	-	m^2
A_{RR}	Area of removed region	*ARR*	cm^2
A_{TF}	Theoretical final area of covered region	*FACR*	cm^2
A_{TI}	Theoretical initial area of covered region	*IACR*	cm^2
C	Percentage of dead space in compressor	-	%
D_N	Nozzle diameter	*NOD*	mm
$D_{N\text{-}S}$	Distance between nozzles and sunflower head	*DNS*	mm
D_T	Theoretical diameter of initial covered region	*DICR*	mm
k	Specific heat transfer	-	-
L	Lubrication factor	-	-
$\dot{m}$	Mass flow rate in nozzle exit	-	kg s^{-1}
P	Air pressure at the nozzle exit	-	Pa
P_1	Pressure in input of compressor	-	Pa
P_2	Pressure in output of compressor	-	Pa
P_c	Power consumption	*PWR*	kW or hp
R	Real gas constant equals 8.314472	-	J K^{-1} mol^{-1}
T	Temperature	-	K
U_0	Uniform initial velocity of air in the nozzle outlet	-	m s^{-1}
U_m	Main velocity of air in the nozzle outlet		m s^{-1}
V_L	Linear velocity of conveyor chain	*LVS*	cm s^{-1}
V_{IS}	Local speed of sound	-	m s^{-1}
V_R	Rotational velocity of nozzle	*RV*	rpm
Z	Compressibility factor of air	-	-
Z_1	Compressibility factor of air in input of compressor	-	-
Z_2	Compressibility factor of air in output of compressor	-	-
γ	Polytrophic specific heat transfer	-	-
η_M	Mechanical efficiency	-	%
η_P	Polytrophic efficiency	-	%
η_R	Removing efficiency	-	%
η_V	Volumetric flow efficiency of compressor	-	%
ρ_s	Density of supply air	-	kg m^{-3}